Nuclear Instruments and Methods in Physics Research B 365 (2015) 457–461

Contents lists available at ScienceDirect

Nuclear Instruments and Methods in Physics Research B

journal homepage: www.elsevier.com/locate/nimb

Evaluation of the effective solid angle of a hemispherical deflector analyser with injection lens for metastable Auger projectile states

E.P. Benis [a,*], S. Doukas [b], T.J.M. Zouros [c,d], P. Indelicato [e], F. Parente [f], C. Martins [f], J.P. Santos [f], J.P. Marques [g]

[a] Department of Physics, University of Ioannina, GR 45110 Ioannina, Greece
[b] Department of Material Science and Engineering, University of Ioannina, GR 45110 Ioannina, Greece
[c] Department of Physics, University of Crete, P.O. Box 2208, GR 71003 Heraklion, Greece
[d] Tandem Accelerator Laboratory, INPP, NCSR Demokritos, GR 15310 Ag Paraskevi, Greece
[e] Laboratoire Kastler Brossel, ENS, CNRS, Sorbonne Universités, UPMC, Case 74; 4, place Jussieu, 75252 Paris CEDEX 05, France
[f] LIBPhys-UNL, Dep. Física, FCT, Universidade NOVA de Lisboa, 2829-516 Caparica, Portugal
[g] BioISI – Biosystems & Integrative Sciences Institute, Faculdade de Ciências da Universidade de Lisboa, Campo Grande, C8, 1749-016 Lisboa, Portugal

ARTICLE INFO

Article history:
Received 20 May 2015
Received in revised form 5 July 2015
Accepted 7 July 2015
Available online 14 July 2015

Keywords:
Hemispherical deflection analyzer
Effective solid angle
Metastable states
SIMION

ABSTRACT

The accurate determination of the electron yield of a metastable projectile Auger state necessitates the careful evaluation of the corresponding effective solid angle, i.e. the geometrical solid angle convoluted with the decay time of the metastable state. Recently, we presented (Doukas et. al., 2015) SIMION Monte Carlo type simulations of the effective solid angle for long lived projectile Auger states (lifetime $\tau \sim 10^{-9}$–10^{-5} s) recorded by a hemispherical spectrograph with injection lens and position sensitive detector in the direction of the projectile ion. These results are important for the accurate evaluation of the $1s2s2p\ ^4P/^2P$ ratio of K-Auger cross sections whose observed non-statistical production by electron capture into He-like ions, recently a field of interesting interpretations, awaits final resolution. Here we expand and systematize our investigation using the same techniques to expose universal behaviors of the effective solid angle covering life times of $1s2s2p\ ^4P$ states for all first row ions. Our results are also compared to purely geometrical calculations of the solid angle that omit the lensing effects and serve as a benchmark for a deeper insight into the effect.

1. Introduction

High resolution Auger electron spectroscopy and in particular zero-degree Auger projectile spectroscopy (ZAPS) has made considerable progress in obtaining information on both the atomic structure and the collision dynamics of multiply excited atomic states over the last few decades [1,2]. A persistent problem in such measurements is the determination of the contribution from metastable states to the measured Auger electron yields due to their inherent long lifetime. Indeed, in ZAPS setups, where the electron spectrometer lies in the path of the projectile and the electrons are measured at 0° with respect to the beam direction, the excited metastable projectile states decay all along the ion path towards the spectrometer and therefore the overall electron detection solid angle varies significantly with the position of electron emission resulting in an important correction to the measured 0° electron yield. Until recently, this correction has been treated purely geometrically, by computing the subtended solid angle averaged over the path length and weighted by the time decay of the metastable state [1,3,4]. Such an approach can be in principle applied only to spectrometers that do *not* have focusing elements at their entrance. Thus, spectrographs equipped with a focusing/pre-retardation entry lens, as for example state-of-the-art hemispherical deflector analyzers (HDA) [5], do not allow for such a straightforward geometrical correction treatment of the solid angle.

Recently, we published an investigation based on a Monte Carlo type calculation within the SIMION 8.1 [6] charged particle optics simulation environment to treat the problem of the accurate determination of the solid angle correction factor for our HDA which has a 4-element injection lens [7–10] and also uses a 2-dimensional position sensitive detector (PSD) instead of an exit slit [11]. In this report, we expand and systematize our investigation on the effective solid angle utilizing the same SIMION Monte Carlo approach to expose universal behaviors covering the life times of $1s2s2p\ ^4P$ states for all first row ions. In our results we also include purely geometrical correction calculations that omit the lensing effects

* Corresponding author.

http://dx.doi.org/10.1016/j.nimb.2015.07.006
0168-583X/

and serve as a benchmark for a deeper insight into the correction problem.

Such studies are important in the accurate determination of the electron yield of all metastable states. A particular well-known example is the $1s2s2p\ ^4P$ state whose production has been studied by ZAPS for many processes [1,3,12–17]. Recently, this state has again attracted interest in its formation by electron capture in collisions of He-like ions with various targets [4,18–21]. In particular, the ratio $R = 1s2s2p\ ^4P/^2P$ of cross sections, expected by statistical arguments to have the value of $R = 2$, has been reported to have much larger measured values [18,19], lending itself to various explanations as to the involved mechanisms [19–21]. Clearly, the accurate determination of the effective solid angle is very important in the correct evaluation of R.

2. The correction factor G_τ

The detailed mathematical simulation of the correction factor G_τ has been presented in Ref. [11] and can be summarized as follows: Initially, a realistic extended source is assumed representing the gas cell where all the projectile states are populated in collisions of the incoming ion beam with the gas target. The projectile states are then allowed to decay starting from the production point inside the gas cell up to the area of the spectrometer entry, which in our case coincides with the entrance of the focusing/deceleration lens as illustrated in Fig. 1. Therefore, since the source of electron emission extends over the path of the ion on its way to the spectrometer, the solid angle varies depending on two terms: (i) the geometrical term, resulting in an increase of the acceptance solid angle for projectiles decaying closer to the lens entrance, and (ii) the temporal term, resulting in a decrease of the population of the excited projectiles along the projectile path towards the spectrometer. In this geometry, the solid angle is termed *effective* to distinguish it from the solid angle of a point source.

Thus, the effective solid angle for a metastable state moving with projectile ion velocity V_p with life time τ averaged over the length L_c of the gas cell is written [11]

$$\overline{\Delta\Omega}(L, V_p\tau, L_c) \equiv \left[\frac{1}{L_c}\int_{z'=0}^{L_c} dz' \int_{z=0}^{L-z'} dz \frac{e^{-z/V_p\tau}}{V_p\tau}\Delta\Omega_0(L - z' - z)\right] \quad (1)$$

where L is the maximal distance along the ion trajectory over which significant contributions to the overall electron line shape can be made and found to be adequately represented by the value $L = s_0 + 6$ mm [11], with s_0 the distance of the center of the gas cell to the lens entry.

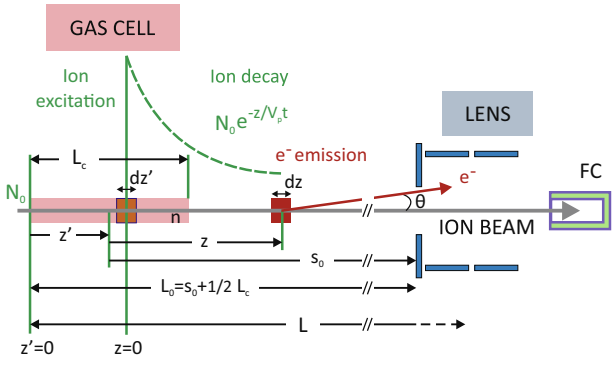

Fig. 1. Schematic of integration region. N_0 ions enter the gas cell (left) with velocity V_p and get excited between z' and $z' + dz'$. Assuming a long life time τ, the excited ionic state travels a further distance z before it decays emitting an Auger electron at angle θ which enters the lens and is eventually energy analyzed by the HDA (not shown). The ions traverse the entire lens and part of the HDA, exiting at the back of the HDA and finally collected in a Faraday cup (FC) used for beam normalization. The length L marks the part of the ion trajectory over which emitted electrons contribute to the Auger line shape with *non-negligible* intensity. L_c denotes the length of the gas cell.

Similarly for a prompt state, i.e. a state with a fast Auger de-excitation that decays entirely inside the gas cell,

$$\overline{\Delta\Omega_0}(s_0, L_c) \equiv \left[\frac{1}{L_c}\int_{z'=0}^{L_c} dz'\Delta\Omega_0(L_c/2 + s_0 - z')\right] \quad (2)$$

where the solid angle $\Delta\Omega_0(s)$ for point source emission into the lens entry aperture of radius r at distance s is given by:

$$\Delta\Omega_0(s) = 2\pi(1 - \cos\theta) = 2\pi\left(1 - \frac{s}{\sqrt{r^2 + s^2}}\right) \quad (3)$$

Then, the correction factor G_τ for the effective solid angle for a certain long-lived Auger state is simply the ratio between the effective solid angle of the metastable state to that of the same, but as if it was *prompt*, i.e.

$$G_\tau = G_\tau(L, V_p\tau, s_0, L_c) \equiv \overline{\Delta\Omega}(L, V_p\tau, L_c)/\overline{\Delta\Omega_0}(s_0, L_c) \quad (4)$$

Here we evaluate this ratio using the SIMION Monte Carlo approach since the focusing element of our spectrograph does not allow for a straightforward geometrical estimation as opposed to spectrometers without focusing elements at their entry. The approach is detailed in Ref. [11]. In brief, at each point of the cylindrical shape ionic trajectory z, a number of emitted electrons is determined according to the product of the temporal term and the geometrical term in Eq. (1) and then multiplied by a starting indicative number N_i that determines the total number of electrons to be flown. The simulated electrons are emitted from ions having kinetic energies between 0.5 and 2 MeV/amu and an Auger energy of 229.64 eV corresponding to the C^{3+} $(1s2s2p\ ^4P)$ state decaying to the C^{4+} $(1s^2)$ ground state. Then the laboratory kinetic energy of the Auger electron is determined according to velocity addition kinematics [11]. Moreover, the electrons are emitted within a cone distribution angle θ defined either by the lens aperture of radius r at distance s or the maximum kinematically allowed angle θ_{max} if the computed θ is found to be larger than θ_{max}. Only monoenergetic electrons were utilized since the width of the metastable states is very small (<μeV) and can be safely neglected in this study. The lifetime τ, depending on the J-substate and ion species lies between 0.1 and ~6500 ns, is assigned to each generated electron group. The chosen temporal range is in accordance to the realistic lifetimes of the $1s2s2p\ ^4P_j$ (J = 1/2, 3/2, 5/2) for atomic numbers $3 \leqslant Z \leqslant 10$. Indeed, in Table 1, we present the results of theoretical calculations performed for the above cases including the Auger and X-ray rates.

The bound and continuum state wavefunctions, used to calculate the radiative and radiationless decay rates, were provided by the multi-configuration Dirac–Fock (MCDF) code of Desclaux and Indelicato [22,23]. The code was used in the single-configuration approach, with the Breit interaction and the vacuum polarization terms included in the self-consistent field calculation, and other QED effects, such as self-energy, included as perturbations [24,25]. The radiationless transitions were analysed considering a two-step process, in which the decay is independent from the capture event. Thus, the two electrons do not interact with each other and the core hole state interacts very weakly with the continuum electron, allowing for the transition rates to be calculated from perturbation theory. The continuum-state wavefunctions were obtained by solving the Dirac–Fock equations using the atomic potential of the initial state, and were normalized to represent one ejected electron per unit energy.

Noticing that the two variables, V_p and τ, appear as a product in Eq. (1) we performed the study as a function of the universal variable $V_p\tau$ which has dimensions of length and thus can be

Table 1
Theoretical calculations of Auger rates W_A, X-ray rates W_X and lifetimes τ of the $1s2s2p\ ^4P_j$ states (J = 1/2, 3/2, 5/2) for atomic numbers $3 \leqslant Z \leqslant 10$. Numbers in square brackets stand for powers of 10.

Z	$^4P_{1/2}$			$^4P_{3/2}$			$^4P_{5/2}$		
	W_A (s^{-1})	W_X (s^{-1})	τ (ns)	W_A (s^{-1})	W_X (s^{-1})	τ (ns)	W_A (s^{-1})	W_X (s^{-1})	τ (ns)
3	8.93[6]	2.43[2]	112.04	4.81[6]	7.37[2]	207.66	1.56[5]	1.38[1]	6396.90
4	4.98[7]	1.19[4]	20.08	2.51[7]	3.32[4]	39.82	9.40[5]	3.52[2]	1062.98
5	1.51[8]	1.78[5]	6.62	6.85[7]	4.79[5]	14.49	3.23[6]	3.35[3]	308.89
6	3.39[8]	1.45[6]	2.94	1.37[8]	3.83[5]	7.10	8.22[6]	1.91[4]	121.36
7	6.43[8]	8.11[6]	1.54	2.23[8]	2.12[7]	4.10	1.76[7]	7.95[4]	56.46
8	1.08[9]	3.49[7]	0.90	3.09[8]	9.06[7]	2.50	3.36[7]	2.66[5]	29.57
9	1.66[9]	1.24[8]	0.56	3.64[8]	3.21[8]	1.46	5.87[7]	7.56[5]	16.83
10	2.41[9]	3.80[8]	0.36	3.90[8]	9.85[8]	0.73	9.52[7]	1.91[6]	10.29

straightforwardly compared to the dimensions of the setup. Indicative results are presented in Fig. 2. We focused our study on usual operating conditions of our spectrometer corresponding to deceleration factors $F = 4$ and $F = 8$. The experimental setup simulated is presently located at the 5 MV tandem accelerator facility of the NCSR Demokritos in Athens, Greece [26], for which the length of the gas cell is $L_c = 50$ mm, the distance of the center of the gas cell from the lens entry is $s_0 = 289$ mm and the radius of the lens entry aperture is $r = 2$ mm. For clarity the $V_p\tau$ axis is plotted in log scale. It is seen that the value G_τ increases rapidly for distances up to about 200 mm and then drops off much slower over distances that may reach meters.

This can be qualitatively understood as follows: Small $V_p\tau$ values, i.e. $V_p\tau \ll s_0$, practically correspond to short decay times τ. Thus, the majority of the excited ions decay well before they reach the lens entrance. Therefore the temporal term can be considered constant and the correction factor G_τ increases solely due to the increase of the solid angle, i.e. the geometrical term. On the other hand, for large decay times, i.e. $V_p\tau \gg s_0$ the situation is inverted. Most of the ions decay after they enter the lens all the way through the spectrometer and possibly even after exiting it in the back. In this case, the geometrical term is constant, while the temporal term is decreasing exponentially and thus the effective solid angle and therefore the correction factor G_τ follow the exponential decay pattern observed in the simulations. For intermediate decay times, $V_p\tau$ and s_0 are of the same order, as are the temporal and geometrical terms, resulting in a maximum observed in our case around 200 mm after the gas cell center.

The same behaviour was observed for the case of deceleration factor $F = 8$ although a decrease of about 30% for the larger values of G_τ is evident. This decrease is attributed to the higher deceleration conditions. Higher deceleration is necessary for achieving improved energy resolution, however, it usually comes at the expense of electron transmission even for spectrographs equipped with a focusing/decelerating lens at their entrance. The reason is that even for prompt states higher deceleration conditions allow for much smaller angles θ to be transmitted than the maximum angle θ_{max} allowed by the geometry with no deceleration. SIMION simulations for deceleration factors $F = 4$ and $F = 8$ for both prompt and metastable states are presented in Fig. 3. Assuming an ion beam energy of 1 MeV/amu ($V_p = 13.89$ mm/ns) and an Auger energy of 229.64 eV, it is seen that the *prompt* state, when detected at $F = 4$, has a detection efficiency *larger* by a factor of 1.85 compared to that for $F = 8$. Similarly, for a *metastable* state having a lifetime of $\tau = 10$ ns and $V_p\tau = 138.9$ mm, the detection efficiency for $F = 4$ remains not only higher than that for $F = 8$ after multiplying

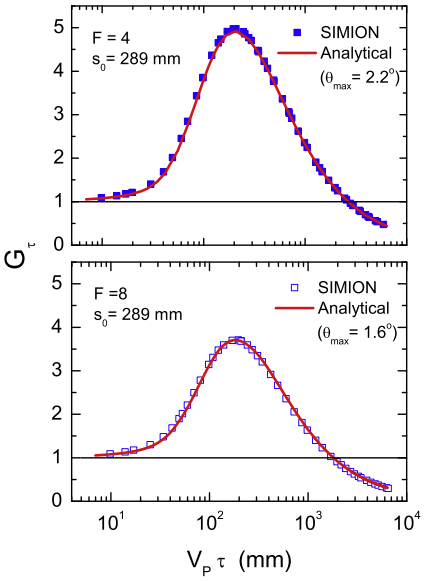

Fig. 2. The effective solid angle correction factor G_τ is plotted as a function of the universal parameter $V_p\tau$, where V_p is the projectile velocity and τ the lifetime of the state. [Top] Deceleration factor F = 4. [Bottom] Deceleration factor $F = 8$. The solid lines represent analytical calculations based on Eqs. (1)–(4) limited to maximum angles $\theta \leqslant \theta_{max} = 2.2°$ for F = 4 and $\theta_{max} = 1.6°$ for $F = 8$ for which the analytical results scale exactly to the SIMION simulation results. s_0 is the distance of the target gas cell center to the lens entry of the spectrograph.

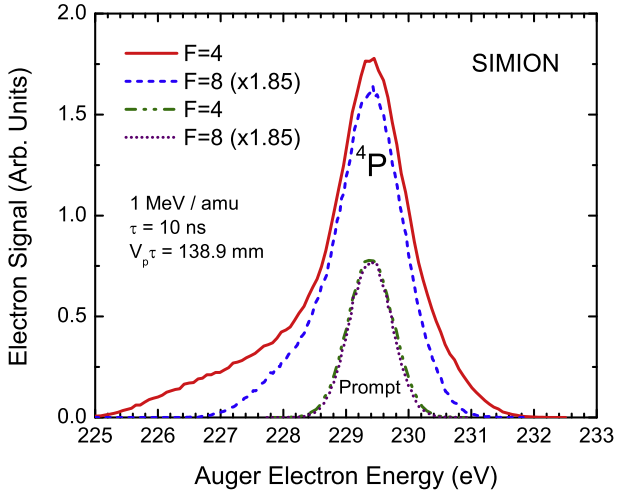

Fig. 3. Comparison of line profiles and overall detection efficiencies for prompt and metastable states at deceleration factor $F = 4$ and $F = 8$ for an ion beam energy of 1 MeV/amu and an Auger energy of 229.64 eV. For very short lifetimes (prompt states) the line profiles are seen to be practically identical in shape for either $F = 4$ or $F = 8$. However, the detection efficiency is higher for $F = 4$ by a factor of 1.85. For much longer lifetimes (metastable states) with $\tau = 10$ ns and $V_p\tau = 138.9$ mm, the detection efficiency for $F = 4$ is seen to be slightly higher than that for $F = 8$, while the line profiles for $F = 4$ are seen to be much broader than for $F = 8$.

by 1.85, but is seen to even have a quite different spectral distribution. The lower, and to a lesser extent, the higher energy wings are clearly narrower for $F = 8$. The lower energy asymmetric part corresponds kinematically to larger angles θ [11] that depart from paraxial values necessary for the $F = 8$ deceleration conditions and thus are filtered out of the peak area by the entry lens.

It should be emphasized that the above results depend somewhat on the focusing conditions, i.e. on the particular lens voltages utilized. In this study for both cases *optimum* lens voltages were utilized determined either experimentally in the case of $F = 4$ or via SIMION simulations in the case of $F = 8$. By optimum we mean the voltages that result in the optimal (i.e. highest) spectrograph energy resolution.

Going one step further, in order to obtain a deeper understanding of the functional behavior of G_τ, we performed analytical calculations based on Eqs. (1)–(4) using the Mathematica package. These calculations do not depend on the deceleration factor since they only depend on geometrical and temporal parameters. In our approach we restricted the solid angle to a smaller maximum value θ_{max}. Since θ_{max} is defined by the radius of the lens entry aperture r and the point of emission, we adjusted r accordingly to selectively limit the value of θ_{max}. We then varied θ_{max} so to match the analytical result to the SIMION result at the maximum G_τ value. We, thus, obtained the value of $\theta_{max} = 2.2^\circ$. After repeating these calculations for all the values of the variable $V_p\tau$ we found, to our surprise, that they accurately reproduced our SIMION results. Similar results, but for an angle of $\theta_{max} = 1.6^\circ$ were obtained for the case of $F = 8$ as illustrated in Fig. 3 by the solid lines. This outcome strongly indicates that only a narrow range of θ angles ($\theta \lesssim \theta_{max}$) is detected, while all higher values are filtered out by the spectrometer focusing/deceleration elements.

We attempted to verify the above analytical result by repeating the same θ_{max} study in the SIMION environment. We compared the $1s2s2p\ ^4P$ metastable peak spectral distribution for various θ_{max} angles to that of the maximum kinematically allowed value of $\theta_{max} = 40.3^\circ$ [11]. As shown in Fig. 4, the metastable peak distribution was accurately reproduced for $\theta_{max} = 2.0^\circ$ in excellent agreement with the previous analytical calculations. This unexpected finding is of great importance for two reasons: Firstly, it provides a detailed insight into the angle filtering action imposed by the focusing/deceleration process. Secondly, it also provides an accurate value for the correction factor G_τ even when obtained by the analytical calculation. Even if SIMION is used, the solid angle can be restricted to much smaller values than the kinematically allowed, resulting in a dramatic decrease in the overall large simulation time.

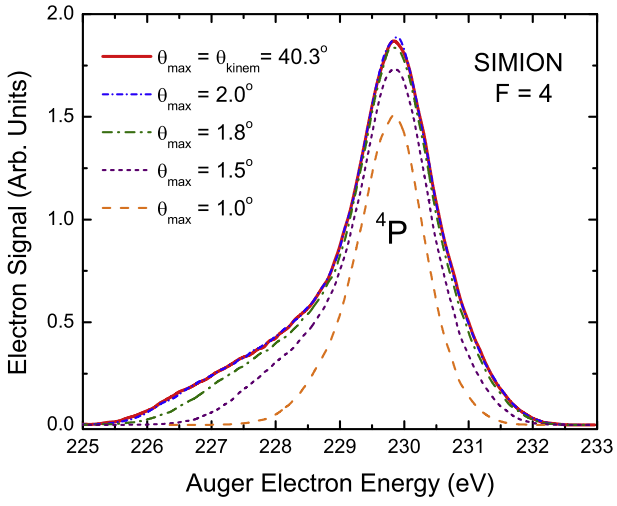

Fig. 4. Comparison of the $1s2s2p\ ^4P$ metastable state line profile computed by SIMION for different values of θ_{max} angles including the maximum kinematically allowed value of $\theta_{max} = 40.3^\circ$ for the parameters of Fig. 3. The line profile for $\theta_{max} = 2^\circ$ is seen to be near agreement with that for $\theta_{max} = 40.3^\circ$. These results are also in excellent agreement with analytical calculations.

3. Summary and conclusion

In this work we report on an extended investigation of the effective solid angle correction for a hemispherical deflector analyser with injection lens for metastable projectile Auger electrons. Utilizing a SIMION 8.1 Monte Carlo type simulations approach we have determined the correction factor's dependence on the universal parameter $V_p\tau$, i.e. the product of the projectile velocity V_p and the lifetime of the metastable state τ, at typical deceleration conditions of $F = 4$ and $F = 8$. Our SIMION investigations show that only solid angles corresponding to $\theta \lesssim \theta_{max} = 2^\circ$ contribute to the overall detected Auger yield for the metastable states, while higher values are filtered out by the injection lens. Once the appropriate much smaller limiting angle θ_{max} has been determined it can be used in our analytical calculations which are then in agreement with our SIMION, a fact of immediate practical importance since we may now use the much faster analytic calculations of the effective solid angle correction for such spectrometers. These calculations are important for obtaining accurate correction factors for use in the determination of the electron yield of metastable states, as for example the ratio $R = 1s2s2p\ ^4P/^2P$ of recent interest as large departures from the expected statistical value of $R = 2$ have been reported.

Acknowledgements

This investigation was partially co-financed by the European Union (European Social Fund-ESF) and Greek national funds through the Operational Program Education and Lifelong Learning of the National Strategic Reference Framework (NSRF)-Research Funding Program: THALES. Investing in knowledge society through the European Social Fund (Grant No. MIS 377289).

References

[1] T.J.M. Zouros, D.H. Lee, Zero degree auger electron spectroscopy of projectile ions, in: S.M. Shafroth, J.C. Austin (Eds.), Accelerator-based Atomic Physics Techniques and Applications, American Institute of Physics Conference Series, Woodbury, NY, 1997, pp. 426–479. Ch. 13.
[2] N. Stolterfoht, R.D. Dubois, R.D. Rivarola, Electron Emission in Heavy Ion-atom Collisions, Springer Series on Atoms and Plasmas, Berlin, 1997.
[3] D.H. Lee, T.J.M. Zouros, J.M. Sanders, P. Richard, J.M. Anthony, Y.D. Wang, J.H. McGuire, Phys. Rev. A 46 (1992) 1374.
[4] J.A. Tanis, A.L. Landers, D.J. Pole, A.S. Alnaser, S. Hossain, T. Kirchner, Phys. Rev. Lett. 92 (13) (2004) 133201.
[5] T.J.M. Zouros, E.P. Benis, Appl. Phys. Lett. 86 (2005) 094105.
[6] SIMION Version 8.1.2.20, Scientific Instrument Services, Ringoes, NJ, 2014, see <http://www.simion.com>.
[7] E.P. Benis, K. Zaharakis, M.M. Voultsidou, T.J.M. Zouros, M. Stöckli, P. Richard, S. Hagmann, Nucl. Instr. Meth. Phys. Res. B 146 (1998) 120–125.
[8] E.P. Benis, T.J.M. Zouros, P. Richard, Nucl. Instr. Meth. Phys. Res. B 154 (1999) 276–280.
[9] E.P. Benis, T.J.M. Zouros, Nucl. Instr. Meth. Phys. Res. A 440 (2000) 462–465.
[10] E.P. Benis, T.J.M. Zouros, J. Electron Spectrosc. Relat. Phenom. 163 (2008) 28–39.
[11] S. Doukas, I. Madesis, A. Dimitriou, A. Laoutaris, T.J.M. Zouros, E.P. Benis, Rev. Sci. Instr. 86 (4) (2015) 043111.
[12] T.J.M. Zouros, D.H. Lee, P. Richard, Phys. Rev. Lett. 62 (1989) 2261.
[13] D.H. Lee, P. Richard, J.M. Sanders, T.J.M. Zouros, J.L. Shinpaugh, S.L. Varghese, Nucl. Instr. Meth. Phys. Res. B 56 (57) (1991) 99.
[14] T.J.M. Zouros, D.H. Lee, P. Richard, J.M. Sanders, Nucl. Instr. Meth. Phys. Res. B 56 (57) (1991) 107.
[15] T.J.M. Zouros, B. Sulik, L. Gulyás, A. Orbán, J. Phys. B 39 (2006) L45–L52.
[16] E.P. Benis, T.J.M. Zouros, T.W. Gorczyca, A.D. González, P. Richard, Phys. Rev. A 73 (2006) 029901(E).
[17] T.J.M. Zouros, B. Sulik, L. Gulyás, A. Orbán, Braz. J. Phys. 36 (2006) 505–508.

[18] D. Strohschein, D. Rohrbein, T. Kirchner, S. Fritzsche, J. Baran, J.A. Tanis, Phys. Rev. A 77 (2) (2008) 022706.
[19] T.J.M. Zouros, B. Sulik, L. Gulyas, K. Tokesi, Phys. Rev. A 77 (5) (2008) 050701.
[20] T.J.M. Zouros, B. Sulik, L. Gulyas, K. Tokesi, J. Phys. Conf. Ser. 163 (1) (2009) 012004.
[21] D. Röhrbein, T. Kirchner, S. Fritzsche, Phys. Rev. A 81 (4) (2010) 042701.
[22] J.P. Desclaux, Comp. Phys. Commun. 9 (1) (1975) 31.
[23] P. Indelicato, J.P. Desclaux, Phys. Rev. A 42 (9) (1990) 5139.
[24] J.P. Santos, J.P. Marques, F. Parente, E. Lindroth, P. Indelicato, J.P.J. Phys, B: At, Mol. Phys. 32 (1999) 2089.
[25] M.C. Martins, A.M. Costa, J.P. Santos, F. Parente, P. Indelicato, J. Phys. B At. Mol. Phys. 37 (2004) 3785–3795.
[26] I. Madesis, A. Dimitriou, A. Laoutaris, A. Lagoyannis, M. Axiotis, T. Mertzimekis, M. Andrianis, S. Harissopulos, E.P. Benis, B. Sulik, I. Valastyn, T.J.M. Zouros, J. Phys, Conf. Ser. 583 (2014) 012014.